PHYSICAL REVIEW A VOLUME 16, NUMBER 5 NOVEMBER 1977

Production of orientation and alignment in heavy-ion–surface collisions*

H. G. Berry and G. Gabrielse
Argonne National Laboratory, Argonne, Illinois 60439
and Department of Physics, University of Chicago, Chicago, Illinois 60637

A. E. Livingston
Argonne National Laboratory, Argonne, Illinois 60439
(Received 20 June 1977)

We have measured the alignment and orientation parameters of forward-scattered argon ions excited in grazing-incidence collisions with a Cu surface. The polarization of the light emitted from excited scattered ions has been measured simultaneously with a measurement of their spatial position relative to the interaction region. We have measured the dependence of the orientation with ion energy, incidence angle, scattering angle, and surface material. Total ion angular distributions are found to be independent of incident energies between 0.50 and 3.0 MeV. Possible excitation mechanisms for producing the observed charge states, excited states, alignment, and orientation are discussed. We compare this surface excitation with the excitation of ions passing through thin foils.

I. INTRODUCTION

Recent experiments[1,2] have shown that ions undergoing grazing-incidence collisions at clean metal surfaces are strongly oriented. Circular polarization fractions of up to 80% have been observed in optical transitions of Ar^+ ions excited at Cu and Au surfaces. The large atomic orientation can be used to study atomic structure parameters such as g-values, fine and hyperfine constants, and also in nuclear-structure measurements.[3] In addition, since the polarization fraction is very sensitive to the scattering angle of the ion-surface collision,[2] such polarization measurements can be used to investigate the collision process itself.

The scattering distributions of charge states and excited-state populations of MeV energy ions from metallic surfaces are essentially unknown. At low energies (a few keV), the elastic scattering component dominates at high angles of incidence (near grazing), giving a forward-peaked outgoing distribution about the specular reflection angle.[4] Recently, Andrä *et al.*[1] have verified that the same types of ion distributions occur for 300-keV Ar^+ ions at angles of incidence more than 80° from the normal. No other measurements of scattered ion distributions have been made for high incidence angles or with other ions in the MeV energy range. The charge-state fractions and excited-state populations have not been measured.

We propose that a final-state ion-surface interaction is the dominant production mechanism of the charge- and excited-state distributions as well as producing alignment and orientation of these excited states. In particular, the orientation, which by symmetry, must be due to a surface interaction, may be comparable to orientation produced in thin-foil excitation. The charge-state and excited-state distributions produced by the ion-surface interaction will also be comparable to those obtained from foil excitation if they are determined by a final-surface interaction.

Excited-state distributions from excitation in thin perpendicular foils have been studied by Veje,[5] who has derived a semiempirical model to fit his results. However, no data are available for tilted foils, and only a few excitation functions in helium and lithium have been measured for different material foils.[6] The distributions from surfaces are completely unknown.

In this paper we present polarization measurements of surface-scattered ions which help to analyze the collision processes. We have measured the linear and circular polarization fractions as spatial distributions about the scattering surface. We are able to interpret these results in terms of the polarization fractions of photons from particles leaving the surface at different angles. These polarizations can then be compared with those obtained from excitation in thin, tilted carbon foils.[7] By measuring at different effective observation angles, we can deduce the complete set of alignment and orientation parameters for the excited states. In particular, for the forward-scattered ions, these results establish some unusual characteristics of the final-state interaction. We have also measured the variations of the polarization fractions with incidence angle, ion-beam energy, and surface material. Finally we discuss the validity of various possible interaction mechanisms for the surface-scattering process.

II. EXPERIMENT

The experimental geometry is shown in Fig. 1. The target was electrically isolated at +300 V and the net collected current was used as a normalizing signal. Two target arrangements were used. In the first arrangement the target was at fixed Z position, but could be rotated about the x axis (angle α). Photon observations were made only in the x direction ($\phi = 0$). The optical system was focused in the interaction plane at a particular ($x = 0, y, z$) position which could be adjusted in the y and z directions independently. In the second arrangement, the target was held at a fixed tilt angle α, was movable along the z axis, and could be rotated about the z axis ($-\phi$ rotation). This target rotation is equivalent to rotating the observation direction in the $+\phi$ sense in the x-y plane: that is, observing the emitted photons $h\nu$ as shown in Fig. 1 at the polar angles ($\theta = 90°, \phi$). Note that the surface tilt angle α to the incident beam is unchanged during the ϕ rotation. The observation point could also be adjusted in the y and z directions independently, as in the first arrangement. The observation image used was generally $\Delta y \approx 1.0$ mm, $\Delta z \approx 0.2$ mm.

Total ion distribution measurements were made using a 1-mm-diam brass rod, parallel to and 50 mm from the x axis of Fig. 1, and rotatable (the angle θ) around the x axis. The current to the pick-up rod, with target and rod biased at 0 and −500 V, respectively, to avoid spurious electron currents, gave the total ion current as a function of angle of scattering θ at the surface. It should be noted that multiply charged ions are not distinguished from singly charged ions in this technique, nor are sputtered ions distinguished from scattered incident ions. For higher angular resolution of the forward-peaked distribution which occurred for small grazing angles, the ion-collection-rod axis was moved down beam from the target, increasing the effective angular resolution to better than 3 mrad.

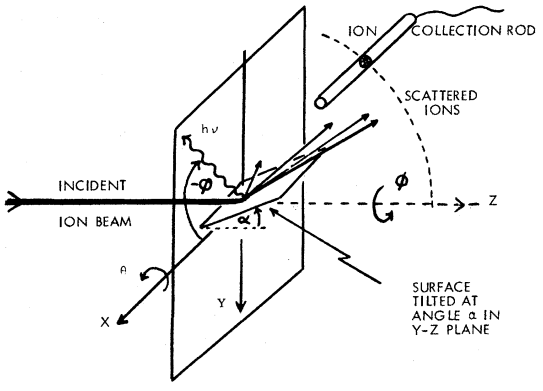

FIG. 1. Experimental geometry. The surface normal is in the Y-Z plane, tilted at an angle α to the Y axis. The ion collection rod is parallel to and rotates about the X axis. The incident beam is collimated to a 1 mm height in the Y direction, 5 mm in the X direction, and a divergence of less than 6 mrad.

The light was observed through a polarization-analysis system[8] with a $\frac{3}{4}$-m Czerny-Turner monochromator equipped with a Bailey Centronic 4249 photomultiplier tube and pulse-counting electronics. The polarization system allows simultaneous measurement of the four Stokes parameters I, M/I, C/I, and S/I where I is normalized to the total beam charge. In Fig. 2 we show an example of the measured data, together with its Fourier transform used in obtaining the Stokes parameters.

III. TOTAL ION ANGULAR DISTRIBUTIONS

The angular distributions of fast ions scattered by metallic surfaces have not been measured or calculated for energies in the range above a few hundred keV. In our measurements we have used Ar^+ ions incident at energies from 0.6 to 3.0 MeV on a copper surface at incidence angles between 76° and 89°. For these incidence angles ($90° - \alpha$), the angular distribution is almost independent of the incident-ion energy. In Fig. 3 we show representative angular distributions for the tilt angles

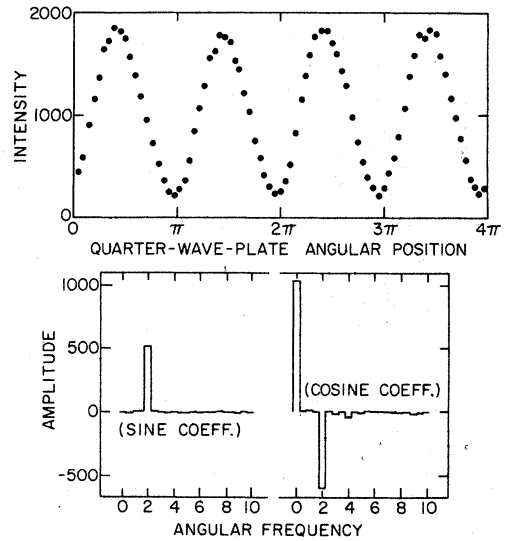

FIG. 2. Observed light yield from the Ar II 4610-Å line excited by a Cu surface at 3° grazing incidence as a function of rotation angle of the retardation plate in the polarization analysis system. In the Fourier transform (lower part) the angular frequencies 2 and 4 correspond to circular and linear polarization components respectively. The derived Stokes parameters are $I = 1021 \pm 5$, $M/I = -0.063 \pm 0.005$, $C/I = 0.012 \pm 0.005$, $S/I = 0.787 \pm 0.006$.

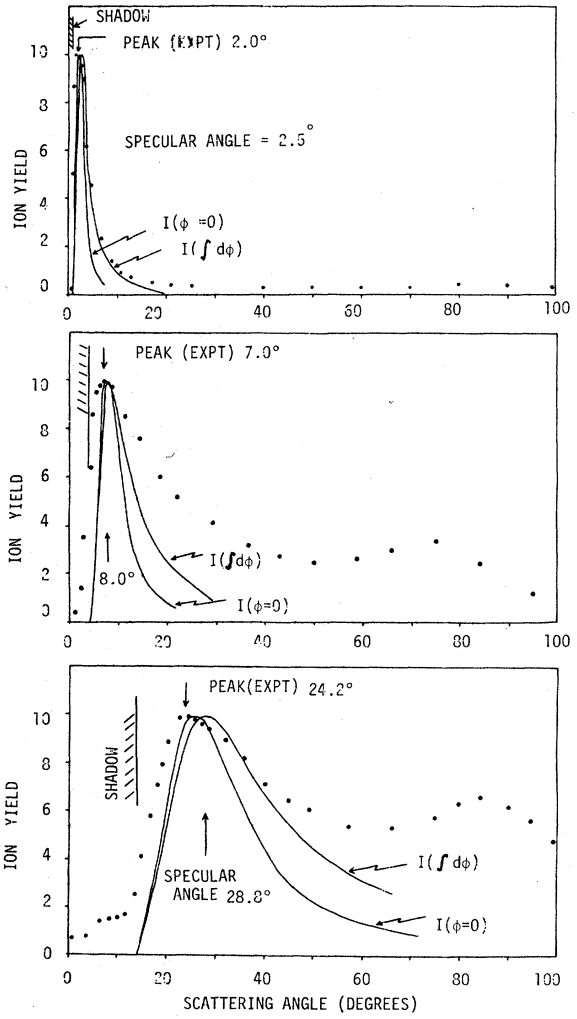

FIG. 3. Ion angular distributions for incidence grazing angles of $\alpha = 1.25°$, 4.0°, and 14.0°.

$\alpha = 1.25°$, 4.0°, and 14.0°. Several useful conclusions may be drawn from these results:

(1) At high angles of incidence, most ions are scattered close to the specular direction, that is, the scattering angle $\theta \approx 2\alpha$. The peak of the angular distribution does not coincide with the specular direction, but appears to be at a slightly more-grazing angle. Thus, for $\alpha = 1.25 \pm 0.25°$, $\theta_{peak} = 2.0 \pm 0.2°$; $\alpha = 4.0 \pm 0.5°$, $\theta_{peak} = 7.0 \pm 0.5°$; and $\alpha = 14 \pm 0.5°$, $\theta_{peak} = 24.2 \pm 0.5°$.

(2) For angles of incidence greater than 87°, the scattered distribution is strongly directed at $\theta \approx 2\alpha$, but the distribution becomes gradually more isotropic for smaller incidence angles. However, the forward-peaked distribution still includes about 55% of the scattered ions for $\theta = 25° \pm 20°$ (half width) with a tilt angle $\alpha = 14°$.

(3) A second peak in the ion distribution occurs near scattering angles of $\theta = 80$–$85°$. This peak is barely visible for low-surface tilt angles (e.g., $\alpha = 1.25°$) and is enhanced at higher tilt angles. The maximum occurs always slightly in the forward direction. Andrä *et al.*[1], in their measurements with 300-keV Ar^+ ions, have suggested that this back peak is due to sputtered surface ions. Although such ions probably contribute to this peak, our optical measurements (below) indicate that there is a significant contribution from back-scattered argon ions even at incidence angles of about 88°. This back peak is slightly enhanced at lower energies relative to the front peak. At very low incident ion energies (of less than 1 keV) this back peak comprises all the scattered ions[9] and has a cosine distribution about the surface normal. Arifov[9] has shown that the double-peak angular distributions of scattered ions are observed for grazing angles of $\alpha = 30°$ for Cs^+ at energies of near 0.5 keV.

As a preliminary model for the scattering of fast heavy ions at the metallic surface, let us assume that the momentum transfer occurs through a series of binary atom-atom collisions at or near the surface. These nearly elastic collisions define a velocity and angular distribution of the scattered ions leaving the surface. Then, the approach to equilibrium in terms of the ion charge state, excited-state distribution, and angular-momentum characteristics, occurs as the ion leaves the surface and will depend on only the outgoing velocity and its direction relative to the surface.

For a single elastic binary collision with scattering through an angle θ, the outgoing velocity is

$$v = \frac{v_0}{1+k}\left[\cos\theta + (k^2 - \sin^2\theta)^{1/2}\right], \tag{1}$$

where $k = M/m$ is the ratio of the mass of the surface atom M to the mass of the incident ion m, which has an initial velocity v_0. Mashkova and Molchanov[4,10] have shown that scattered-ion energies for Ar^+ ions incident on surfaces at 30 keV and grazing angles $\alpha = 5°$–$25°$ show reasonable agreement with such single and double large-angle scatterings. They conclude that a few binary collisions can account for the observed energy distributions. At higher energies, there will be greater penetration into the surface, and more binary collisions will be experienced.[11] However, the velocity distribution of Eq. (1) which is maximized for forward-scattered ions suggests that these ions will have higher velocities than those in the back-scattered peak.

Various observers[12] have shown that single elastic scattering gives a good approximation to the energy dependence of particles as a function of scattering angle, with double and multiple scatter-

ing giving subsidiary energy peaks and broadening, respectively. Parilis and Turaev[13] have calculated the double-scattering case, while multiple scattering from linear chains has been analyzed by Kivilis *et al.*[14] and by Heiland and Taglauer.[15]

The high forward velocities of emission from the surface are expected to yield higher charge-state production at small scattering angles. It is thus surprising to find that the angular distributions (Fig. 3) are independent of energy over the range 0.6 to 3.0 MeV. Multiply charged ions are formed, as shown in the spectra, which are similar to those for thin-foil excited ions of lower incident energy. In Fig. 4, we compare neon spectra from 1.5-MeV incident Ne^+ ions excited from a thin carbon foil and a gold surface (grazing angle $\alpha = 3°$). Although ionization stages II, III, IV, and V are seen in both spectra, the lower stages are enhanced for the surface excitation.

Firsov has calculated the angular distributions of the total reflected particle flux under the assumption of multiple small-angle elastic scattering from an inverse-square-law potential using a diffusion equation for the ions within the solid. For an incident grazing angle α, a total scattering angle θ, and integration over azimuthal angles ϕ, he obtains the flux[16]

$$I_1(\theta,\alpha) = I_0 \frac{\alpha^{1/2}(\theta-\alpha)^{3/2}}{\alpha^3+(\theta-\alpha)^3} . \qquad (2)$$

Firsov has also tabulated[17] a numerical evaluation of flux obtained at zero azimuthal angle $I_2(\theta,\alpha,\phi = 0)$. In our experiment, only ions and not neutral particles are collected, charge states are averaged in proportion to their charge, and the collector integrates over azimuthal angles $-30° \lesssim \phi \lesssim +30°$.

In Fig. 3 we compare the calculated distributions I_1 and I_2 with our experimental distributions. These are the first comparisons with Firsov's theory for scattered particle distributions except for the early work of Mashkova and Molchanov[18] using relatively low-energy 30-keV Ar^+ incident on Cu, W, and graphite. They found the angular distributions to be independent of target material as calculated by Firsov[16, 17] with maxima just below the specular reflection angle $\theta = 2\alpha$. The calculated distributions have maxima for I_1 at $\theta = 2\alpha$ and for I_2 at $\theta = 1.85\alpha$. Since our experiment integrates distributions up to $\pm 30°$ which contains most of the forward-scattered particles, the distribution $I_1(\int d\phi)$ is expected to best represent our results. However, our maximum is close to $\theta = (1.80 \pm 0.05)\alpha$ for all α, more in agreement with $I_2(\phi = 0)$, and the observed angular distribution is broader than that predicted by both calculations. The distributions observed by Mashkova and Molchanov[18] for 30-keV Ar^+ agree closely with our distributions for 0.6–3-MeV Ar^+ for grazing angle $\alpha = 14°$, but their maximum is shifted to high-

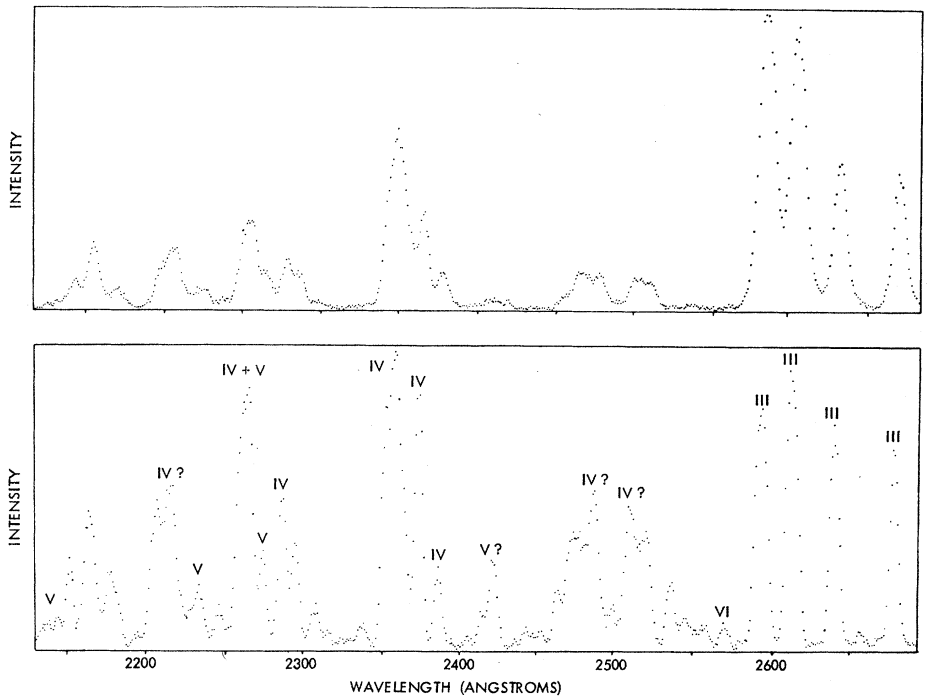

FIG. 4. Neon spectra from a 1.5-MeV incident Ne^+ beam excited by a copper surface at $\alpha = 3°$ (upper) and a perpendicular carbon foil (lower). The charge states of individual components or multiplets are marked where known or suggested from relative intensity measurements.

er scattering angles for small α(e.g., for $\alpha = 4°$, they find $\theta_{max} \approx 10°$). This shift is most probably due to insufficient angular resolution as noted.[18]

Hence, we have the remarkable result that the scattered particle distribution (mostly neutral at 30 keV, mostly ionized at 3 MeV) is independent of incident energy over an energy range of at least two orders of magnitude. This energy independence plus the independence of ion-to-target mass ratio suggests that the small-angle scattering is correctly described by the diffusion theory of Firsov, while the broader distributions show that more large-angle elastic scattering must be included. This last conclusion also agrees with the observations that the energy distributions[11-15] follow from single and double large-angle scattering.

IV. OPTICAL OBSERVATIONS

We are able to learn more about the ion-surface interaction by detecting dipole radiation from collision-excited ions simultaneously with a measurement of the spatial position of the excited ions. We narrow the field of view of our detection optics to a window measuring 1 mm high by 0.2 mm wide (Fig. 1 and Sec. II). By measuring the light polarization at each window position, we are able to learn about the electron-cloud distribution of the collision-excited ions as a function of their spatial position. In this section we begin with a brief review of the atomic information available in dipole radiation. We then describe measurements of atomic alignment and orientation as a function of the position of the surface-scattered ions, showing that atomic orientation is very strongly dependent on ion-scattering angle.[2] We conclude that a final-state interaction between the surface and the scattered ion is responsible for the large orientations.

A. Information available in polarized dipole radiation

Stokes[19] showed that all of the information carried by partially polarized light can be conveniently measured in terms of four numbers, now called Stokes parameters, defined below in terms of the detection coordinate system of Fig. 5:

$$\begin{aligned} I &= \text{total intensity} = I(0°) + I(90°), \\ M &= I(0°) - I(90°), \\ C &= I(45°) - I(-45°), \\ S &= I_{\text{rhc}} - I_{\text{lhc}}. \end{aligned} \tag{3}$$

We use the familiar spherical-coordinate unit vectors generated by the photon wave vector $\vec{k}$ to specify the detection coordinates. The angle Ψ specifies the light polarization axis. The electric dipole radiation from the decay of a coherently excited state of angular momentum F can be described by four independent parameters. Ellis[20] has used the components ρ_{kq} ($k \leq 2$, $|q| \leq k$) of a spherical tensor expansion of the excitation density matrix ρ, while Fano and Macek[21] have defined an orientation parameter O_{1-}^{col} and three alignment components A_0^{col}, A_{1+}^{col} and A_{2+}^{col}. We display below the relationships of these parameters for the case of reflection symmetry across the yz plane.

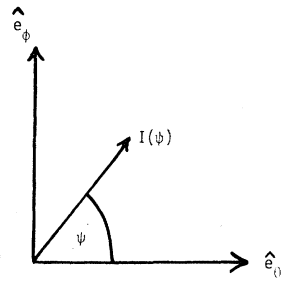

FIG. 5. For photons propagating in the r direction, the intensity vector $I(\Psi)$ is defined by the angle Ψ as shown for the coordinates $(\hat{e}_\theta, \hat{e}_\phi, \hat{e}_r)$.

$$\bar{O}_{1-}^{\text{col}} = O_{1-}^{\text{col}}[F(F+1)]^{1/2} = \frac{\langle F_x \rangle}{[F(F+1)]^{1/2}} = \tfrac{2}{3} R_1(F)[F(F+1)]^{1/2} \frac{\rho_{11}}{\rho_{00}}, \tag{4}$$

$$A_0^{\text{col}} = \frac{\langle 3F_z^2 - F^2 \rangle}{F(F+1)} = -\left(\tfrac{2}{5}\right)^{1/2} R_2(F) \frac{\rho_{20}}{\rho_{00}}, \tag{5}$$

$$A_{1+}^{\text{col}} = -\frac{\langle F_y F_z + F_z F_y \rangle}{F(F+1)} = \frac{2i}{15^{1/2}} R_2(F) \frac{\rho_{21}}{\rho_{00}}, \tag{6}$$

$$A_{2+}^{\text{col}} = \frac{\langle F_y^2 - F_x^2 \rangle}{F(F+1)} = \frac{2}{15^{1/2}} R_2(F) \frac{\rho_{22}}{\rho_{00}}, \tag{7}$$

where

$$R_k(F) = \begin{Bmatrix} 11k \\ FFF \end{Bmatrix} \Big/ \begin{Bmatrix} 110 \\ FFF \end{Bmatrix}. \tag{8}$$

We use the orientation and alignment parameters as defined by Fano and Macek except that we define a renormalized orientation $\bar{O}_{1-}^{\text{col}}$ so that $\bar{O}_{1-}^{\text{col}} = \pm 1$ corresponds to maximum orientation.

When a coherently excited state decays by electric-dipole radiation, the relationships between the measurable photon parameters (the Stokes ratios M/I, C/I, S/I and the total intensity I), and the four atomic parameters (alignment and orientation) are given below, referred to the coordinate system of Fig. 1:

$$M = \tfrac{3}{4} h^{(2)}[A_0^{\text{col}} \sin^2\theta + A_{1+}^{\text{col}} \sin 2\theta \sin\phi - A_{2+}^{\text{col}} (1 + \cos^2\theta)\cos 2\phi], \tag{9}$$

$$C=\tfrac{3}{2}h^{(2)}(A_{1+}^{\mathrm{col}}\sin\theta\cos\phi+A_{2+}^{\mathrm{col}}\cos\theta\sin2\phi), \quad (10)$$

$$S=\tfrac{3}{2}h^{(1)}0_{1-}^{\mathrm{col}}\sin\theta\cos\phi\,, \quad (11)$$

$$I=1-\tfrac{3}{4}h^{(2)}[A_0^{\mathrm{col}}(\cos^2\theta-\tfrac{1}{3})-A_{1+}^{\mathrm{col}}\sin2\theta\sin\phi - A_{2+}^{\mathrm{col}}\sin^2\theta\cos2\phi]. \quad (12)$$

The angles θ and ϕ specify the propagation direction of the detected photon. The detection axis $\hat{e}_\theta$ is parallel to the xy plane in the collision frame. These expressions presuppose that the coherently excited state is produced by a collision process with reflection symmetry across the yz plane. When a transition from an LS-coupled state with angular-momentum quantum numbers LSJ to a state with angular-momentum number J_f is spectroscopically resolved, the geometrical constants $h^{(k)}(J,J_F)$ used by Fano and Macek, modified to include a decoupling, are given by $h^{(k)}(LSJ,J_F)$ where

$$h^{(k)}(LSJ,J_f)=(-1)^k\frac{R_k(J)}{R_k(L)}h^{(k)}(J,J_f)\begin{Bmatrix}L&L&k\\J&J&S\end{Bmatrix}\Big/\begin{Bmatrix}L&L&0\\J&J&S\end{Bmatrix}. \quad (13)$$

This expression assumes a spin-independent excitation process. The alignment and orientation parameters are to be constructed from $\vec{L}$. For the Ar II 4610-Å transition, $4s'\,{}^2D_{5/2}$-$4p'\,{}^2F_{7/2}$, discussed at length in this paper, $h^{(2)}=\frac{10}{7}$ and $h^{(1)}=\frac{27}{7}$.

B. Spatial distribution: Measurements of Stokes parameters

We consider first the intensity and polarization of photons emitted along the x axis ($\theta=90°$, $\phi=0$). Equations (9)–(11) reduce to

$$\frac{M}{I}=\frac{\frac{3}{4}h^{(2)}(A_0^{\mathrm{col}}-A_{2+}^{\mathrm{col}})}{1+\frac{1}{4}h^{(2)}(A_0^{\mathrm{col}}+3A_{2+}^{\mathrm{col}})}, \quad (14)$$

$$\frac{C}{I}=\frac{\frac{3}{2}h^{(2)}A_{1+}^{\mathrm{col}}}{1+\frac{1}{4}h^{(2)}(A_0^{\mathrm{col}}+3A_{2+}^{\mathrm{col}})}, \quad (15)$$

$$\frac{S}{I}=\frac{\frac{3}{2}h^{(1)}0_{1-}^{\mathrm{col}}}{1+\frac{1}{4}h^{(2)}(A_0^{\mathrm{col}}+3A_{2+}^{\mathrm{col}})}. \quad (16)$$

As mentioned previously, we are able to measure simultaneously the light intensity and the Stokes ratios for light coming from excited ions decaying within our detection window. A typical set of measurements is displayed in Fig. 6. The measured photon parameters are plotted above a scaled picture of the detection windows used. The curves measured are smooth within statistical uncertainties.

Figure 6 shows clearly that the Stokes parameter S/I depends strongly on the position of the decaying ion. In terms of the atomic parameters, ions which are forward scattered are highly oriented (i.e., $\langle L_x\rangle$ is large and negative), much like billiard balls striking a cushion. Ions which are scattered into larger angles are less oriented. The intensity maximum and the S/I maximum do not coincide. S/I measured at the intensity maximum would give S/I which is 20% below the maximum value for this example. Because our interaction region was always quite long, considerable averaging over ion-scattering angle is involved in our measurements near the interaction region. However, the measurements down beam from the target are actual angular distributions.

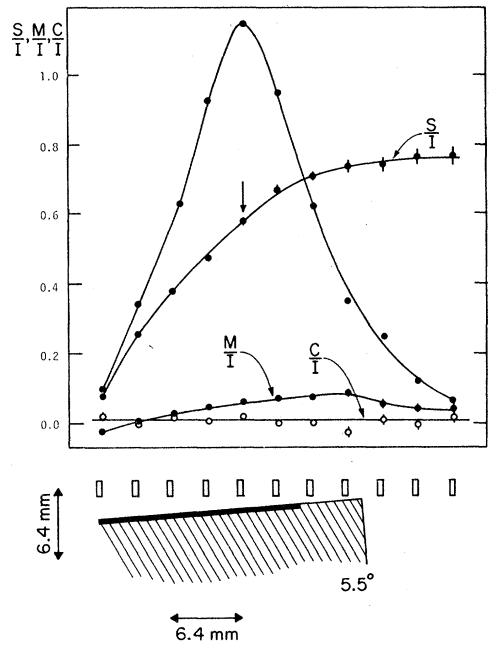

FIG. 6. The lower part shows the geometry for measuring the spatial dependence of the Stokes parameters. Observations at the rectangular detection windows shown gave the Stokes parameter values I, M/I, C/I, and S/I for the Ar II 4610-Å transition shown in the upper figure, the abscissa scale being the same for both parts of the figure.

In Fig. 7 we show a series of measurements at different distances above the interaction region. Notice that the intensity-curve maxima suggest a forward peak in the ion-scattering distribution, consistent with the forward peak discussed earlier in this paper. Ion-velocity distributions must be known for more precise comparisons. We use this data to construct S/I contour plots as shown in Fig. 8. The axes represent distances above and along the target. Obviously we can select any S/I value at all by looking at the appropriate region of space. The S/I values are largest for the forward-scattered ions.

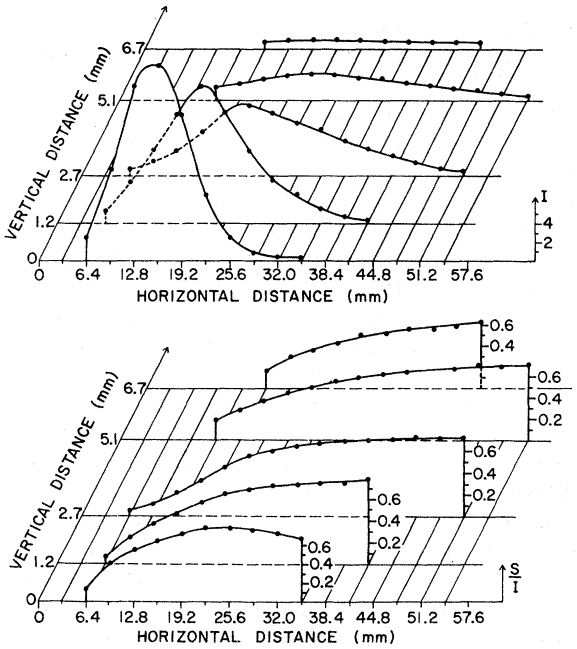

FIG. 7. Series of measurements of I and S/I shown in Fig. 6 at different heights above the tilted copper surface ($\alpha = 5.5°$).

C. ϕ-rotation technique

The light-polarization measurements discussed so far have been for photons emitted along the x axis of Fig. 1. Because we are able to measure only the three Stokes ratios ($M/I, C/I$, and S/I), and not an absolute intensity, we are not able to fully determine the three alignment and one orientation parameters by such a measurement. In an earlier experiment[7] these parameters were determined for a foil-excited ion, by detecting photons emitted in a direction $\theta = 50°$, $\phi = 0°$, in addition to the x-axis photons ($\theta = 90°$, $\phi = 0$). We find it is more convenient to measure photons traveling in the xy plane ($\theta = 90°$). In this case, the effective observation direction can be changed by a rotation ϕ of the target about the beam axis (see Fig. 1). No change of the optical system is thus necessary. Since only a rotation about the z axis is involved, the Stokes parameters depend on angle simply by the factors $\cos(q\phi)$, where q specifies the tensor component.

$$
\begin{aligned}
M &= \tfrac{3}{4} h^{(2)} (A_0^{\mathrm{col}} - A_{2+}^{\mathrm{col}} \cos 2\phi), \\
C &= \tfrac{3}{2} h^{(2)} A_{1+}^{\mathrm{col}} \cos\phi \ , \\
S &= \tfrac{3}{2} h^{(1)} \, 0_{1-}^{\mathrm{col}} \cos\phi \ , \\
I &= 1 + \tfrac{1}{4} h^{(2)} (A_0^{\mathrm{col}} + 3 A_{2+}^{\mathrm{col}} \cos 2\phi) \ .
\end{aligned}
\tag{17}
$$

We illustrate a ϕ-rotation measurement in Fig. 9, for photons from the Ar II 4610-Å transition in the forward-scattered-ion peak, produced by 1.0-MeV Ar^+ ions incident on a copper surface at a grazing angle of 3.5°. We are looking far enough down beam, beyond the target, to ensure that the light comes almost entirely from the forward-scattered ion peak. The S/I and M/I values vary clearly as $\cos\phi$ and $\cos 2\phi$, respectively, suggesting that the denominator of the Stokes ratio equations (9)–(11) is nearly equal to one. The C/I values are consistent with zero. A simple least-squares fit allows us to fully determine the alignment and orientation parameters. We obtain

$$
\begin{aligned}
&A_0^{\mathrm{col}} = -0.109 \pm 0.015, \quad A_{2+}^{\mathrm{col}} = -0.076 \pm 0.015, \\
&A_{1+}^{\mathrm{col}} = 0.00 \pm 0.03, \quad \overline{O}_{1-}^{\mathrm{col}} = -0.421 \pm 0.016.
\end{aligned}
\tag{18}
$$

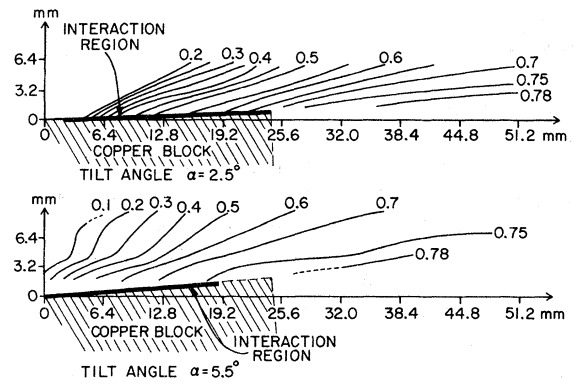

FIG. 8. Contour plots of equal circular polarization S/I of Ar II, 4610-Å for tilt angles of 2.5° and 5.5° of a copper surface. The incident Ar^+ energy was 1.0 MeV.

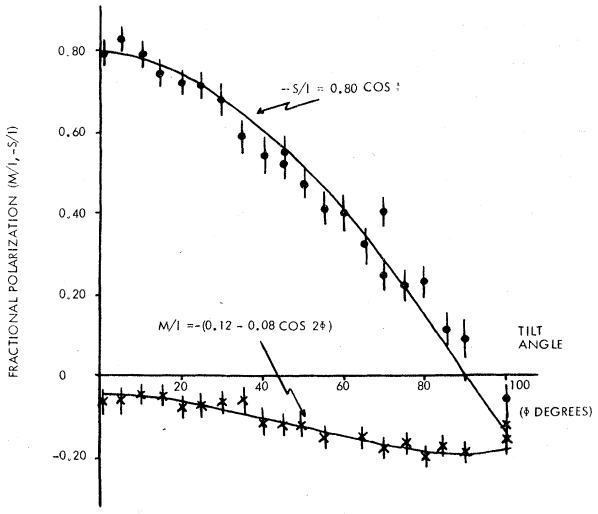

FIG. 9. Variation of the Stokes parameters S/I and M/I of Ar II 4610 Å as a function of the photon emission angle Φ (see Fig. 1). The incident Ar^+ beam of 1.0 MeV was excited by a copper surface at $\alpha = 3°$. The fits to the data (solid lines) follow Eq. (17).

Of course, in most cases it is not necessary to measure such a complete ϕ dependence in order to completely determine these parameters. Measurements at ϕ angles 0°, 45°, and 90° typically suffice. This technique works in principle for any interaction with reflection symmetry, which is studied using subsequent dipole radiation. We have also successfully applied this ϕ-rotation technique to beam-foil interaction studies (work to be published).

D. Description of a state of maximum orientation with no alignment

A pure state can always be constructed which is completely oriented (i.e., $\overline{O}_{1-}^{\mathrm{col}} = \pm 1$). For states with small alignments, however, the maximum allowed orientation is less. Although the orientation and alignment parameters are independent,[21] their maximum allowed values are not.

The S/I measurements reported in Sec. IV B show that the forward-scattered ions have a very large orientation about the x axis (see Fig. 1). Because of the reflection symmetry in the yz plane, the other orientation components are zero. The ϕ-rotation measurements described in Sec. IV C reveal that the ion alignment is very small. These observations lead us to consider a coherently excited state which has the maximum possible orientation consistent with a small amount of alignment.

The density matrix for an oriented state with no alignment, produced by an interaction with reflection symmetry in the yz plane, is given by

$$\rho = [1/(2L+1)]\mathbb{1} + A\vec{L}_x \tag{19}$$

where $\mathbb{1}$ is the unit matrix, and we have assumed that the higher-order multipoles (order > 2) which do not contribute to dipole radiation, are zero. In the (L, L_x) representation, ρ is diagonal. These diagonal elements, being probabilities, must be non-negative, and the $L_x = \pm L$ components give the most restrictive conditions for A, that is,

$$1/(2L+1) \mp AL \geq 0 \tag{20}$$

or

$$|A| \leq 1/L(2L+1) \tag{21}$$

and the maximum orientation is obtained from

$$\langle L_x \rangle = \mathrm{Tr}(\rho L_x) = \tfrac{1}{3} A L(L+1)(2L+1)\,, \tag{22}$$

i.e.,

$$|\overline{O}_{1-}^{\mathrm{col}}| \leq \tfrac{1}{3}(L+1)/[L(L+1)]^{1/2}. \tag{23}$$

This maximum value of the orientation varies only slowly with L, consistent with the measured orientation being almost independent of the multiplet being excited.[1,2]

The limit for the Ar II ^{2}F state (which decays by the 4610-Å transition) is $|\overline{O}_1^{\mathrm{col}}| \leq 0.385$. This is below our observed $\overline{O}_{1-}$ for forward-scattered ions which gave $\overline{O}_{1-}^{\mathrm{col}}$ (expt.) $= -0.421 \pm 0.016$. However, the observed alignments [Eq. (17)] allow the orientation $\overline{O}_{1-}$ to be greater than this limit. The Stokes parameter measurements at $\phi = 0°$ giving M/I close to zero show that $A_0^{\mathrm{col}} \approx A_{2+}^{\mathrm{col}}$, although the measurements at $\phi \neq 0°$ show that A_0^{col} and A_{2+}^{col} are both nonzero and much larger than A_{1+}^{col}. We find from Eq. (17) that the ratio $A_0^{\mathrm{col}}/A_{2+}^{\mathrm{col}} = 1.4 \pm 0.4$. This ratio would be equal to one for no linear polarization in the $\phi = 0$ direction.

If $A_0^{\mathrm{col}} = A_{2+}^{\mathrm{col}}$ and $A_{1+}^{\mathrm{col}} = 0$, the excited-state density matrix is still diagonal in the x representation, with an additional alignment term $B\langle 3L_x^2 - L^2\rangle$ which gives rise to linear polarization when the source is viewed along direction $\phi \neq 0$. Such a state has axial symmetry about the x axis. Our observations of a linear polarization $M/I = -0.20$ at $\phi = 90°$, neglecting the possible contributions due to $M/I = -0.04$ at $\phi = 0°$, raise the maximum allowed orientation from $|\overline{O}_{1-}^{\mathrm{col}}| = 0.385$ to $|\overline{O}_{1-}^{\mathrm{col}}| = 0.53$. This is consistent with our experimental result $\overline{O}_{1-}^{\mathrm{col}} = -0.421$. The higher multipole moments (greater than 2), which have not been measured, may therefore be zero, as assumed in this section.

E. Dependence of polarization on exit angle

The above results have shown that for small incident grazing angles α, the particles scattered in the forward peak near the specular angle $\theta \approx 2\alpha$ show maximum circular polarization. For larger incident grazing angles α, the outgoing particle distribution is not as well defined in scattering angle θ (see Fig. 3), and it is possible to measure more accurately the dependence of the polarizations on the scattering angle for a fixed grazing-incidence angle α. The measurements [Fig. 10A)] were obtained using the geometry shown in Fig. 10(B) and varying the detection window vertically at a position down beam from the target.

The results show that the circular polarization S/I is not a maximum at the specular angle near to the total-intensity maximum, but increases monotonically to the smallest exit-grazing angles. We conclude that the interaction producing the strong circular polarization requires a small grazing angle for the exiting ion, and is, therefore, further evidence of a final-state ion-surface interaction.

F. Dependence of polarization on incident angle

We have measured the circular polarization fraction S/I as a function of surface tilt angle α

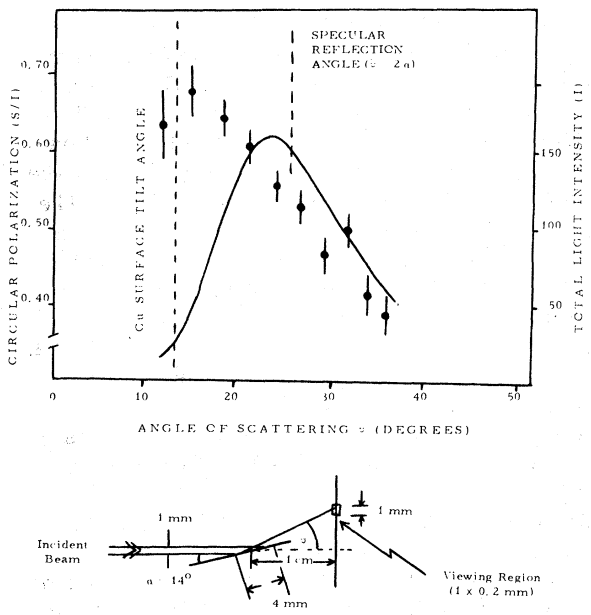

FIG. 10. Circular polarization S/I of Ar II 4610 Å as a function of angle of scattering. The lower part of the figure shows the detection geometry. The total light yield I, the solid line, peaks near the specular reflection angle.

to the incident beam. As Sec. IV E shows a dependence of S/I with exiting angle of the excited ions, each incidence angle can give a range of values for S/I depending on the scattering angle θ. Hence for each incidence angle, we have searched for the maximum S/I for the outgoing ions. For large α (~30°) the measured S/I is an average over many scattering angles. In Fig. 11 we show the spread of S/I values for the forward-scattered ions, and the upper envelope (dotted line) shows that the variation of S/I with α is very small for grazing incidence angles below $\alpha = 10°$. For higher angles α, the light yield comes from ions scattered through large angles of the order of 40 to 60°.

We conclude from the results of Secs. IV E and IV F that the strong circular-polarization-producing interaction is nearly independent of the incident angle and is due to a final-state interaction as the ion leaves the surface at an angle close to grazing. For exit grazing angles less than 10°, S/I varies only slowly with angle.

G. Dependence of polarization on beam energy

We show in Fig. 12 the variation of the circular-polarization fraction S/I of Ar II 4610 Å with incident beam energy for a fixed incident grazing angle $\alpha = 3°$ of a Cu surface. The viewing window is down beam from the interaction region and we are looking at the specularly reflected forward peak. There is only a small dependence of S/I on beam energy, with a small decrease at high energies. Our results extend those of Andrä *et al.*[1] who measured a value of $S/I = 0.76$ for Ar II, 4610 Å after grazing collision with Cu at 300 keV.

Measurements of the incidence-angle dependence of S/I with different incidence energies similarly

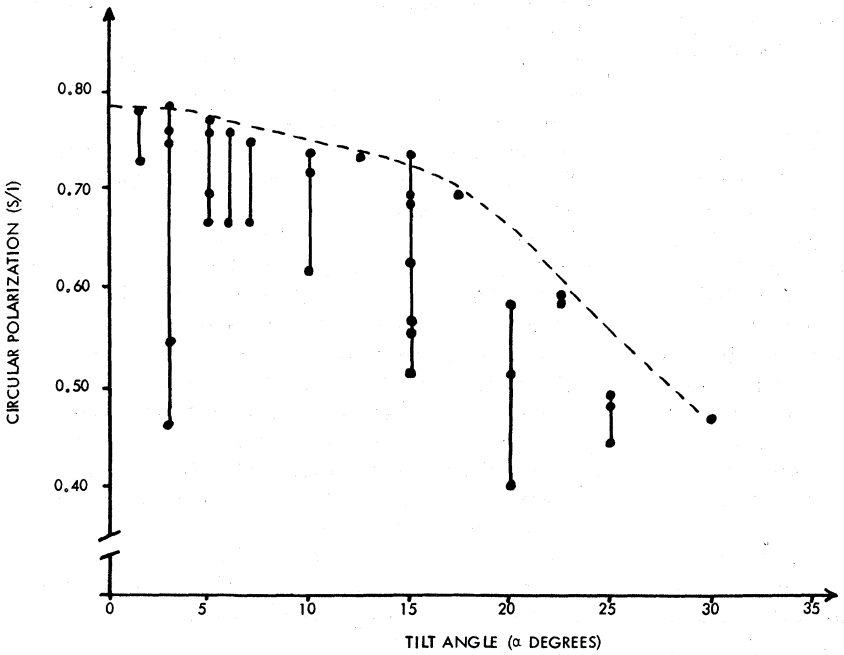

FIG. 11. Circular polarization S/I of Ar II 4610 Å as a function of surface tilt angle α. The different values at each α correspond to observations at different scattering angles θ, the smallest θ giving the highest S/I. The dashed line represents approximate maximum values.

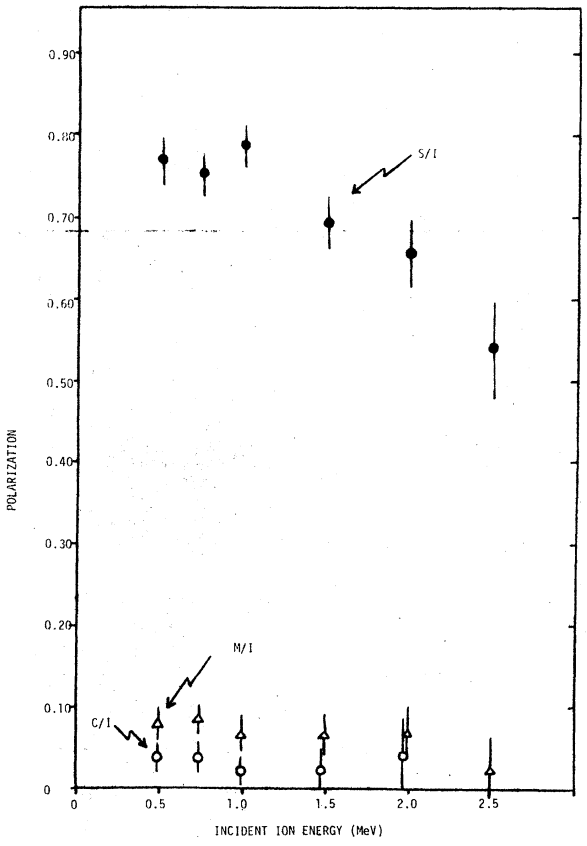

FIG. 12. Stokes parameters for the Ar II 4610-Å transition of the forward-scattered Ar^+ ions excited at a copper surface with 3° grazing incidence angle as a function of incident ion energy.

show only small variations. This can be expected since we have found that the ion distributions are essentially independent of energy.

H. Dependence of polarization on surface structure

The polarization fractions for Ar II, 4610 Å are measured to be similar for "clean" copper and gold surfaces. By "clean" we mean the condition of a polished surface after bombardment of the surface for about one hour with high intensity Ar^+ beams of ~100 $\mu A cm^{-2}$ in a liquid-nitrogen-trapped vacuum of 5×10^{-7} Torr. During this time, as the surface "cleans up", the circular polarization gradually increases to its maximum value of ~0.80. Figure 13 shows the increase in S/I from 0.37 to 0.69 during a bombardment time of 100 min at an observation point close to the interaction region. At the end of this time the forward-scattered ions gave $S/I = 0.80$. However, even though the surface is prepolished to a mirror finish, the beam sputtering during this time produces a granulated surface texture which, although it appears clean, is not microscopically smooth.

Al and Mo surfaces never produced as high S/I of the Ar II 4610-Å transition, but this appeared to be due to the build-up of hydrocarbons on the bombarded surface, even under the same conditions in which Cu and Au remain clean. A graphite surface produced low values of $S/I \approx 0.30$ for the 4610-Å Ar II transition and for the He II transitions $n=3-4$ at 4686 Å and $n=3-5$ at 3204 Å, in agreement with the results of low circular polarizations from metallic surfaces covered with carbon impurities.

V. DOPPLER SHIFTS AND WIDTHS

Measurements of the linewidths and Doppler shifts of the emitted light can provide information on the velocity distributions of the scattered ions. We present here some preliminary measurements which show agreement with the model of the scattered distribution discussed in Sec. III.

For observations in the x direction ($\phi = 0$) of Fig. 1, the major velocity component of the scattered ions will be perpendicular to the optic axis as in the normal beam-foil observations.[22] For the forward-going ions, the geometry is approximately the same as the beam-foil geometry, and we refocused the monochromator[23] to take account approximately of a forward-ion velocity. We show in Fig. 14 the linewidth of the 4610-Å Ar II line as a function of position along the beam axis (z direction of Fig. 1). The peak intensity is at the position of the interaction region. Down beam from this region, the linewidth is smaller showing that the emission comes mainly from ions of a single velocity which has been partially compensated for by the refocusing of the monochromator. At smaller z, the emission occurs from many different velocity ions, causing a larger linewidth.

For observation at angles $\phi \neq 0$, a component of the scattered-ion velocity is along the observation direction, and gives rise to a Doppler shift. Thus, we have compared the wavelengths for the Ar II 4610-Å line of observations of $\phi = 0$ and $\phi = 90°$. We find a wavelength shift to the violet which for 1 MeV incident Ar^+ is 3.0 ± 0.5 Å for a surface tilt angle of $\alpha = 2°$ and 7.0 ± 0.5 Å for $\alpha = 8°$, when viewing down beam from the interaction region. The first result corresponds to ions of 1 MeV at an angle of scattering of $5.0\pm1°$; that is, close to the specular angle. The second result corresponds to specularly reflected ions (at 16°) but with a lower energy of 0.6 ± 0.1 MeV (or ions of higher energy scattered through lower angles).

For angles $\phi \neq 0$, we can determine the scattered-ion velocities which correspond to particular values of the observed Stokes parameters by making polarization measurements as a function

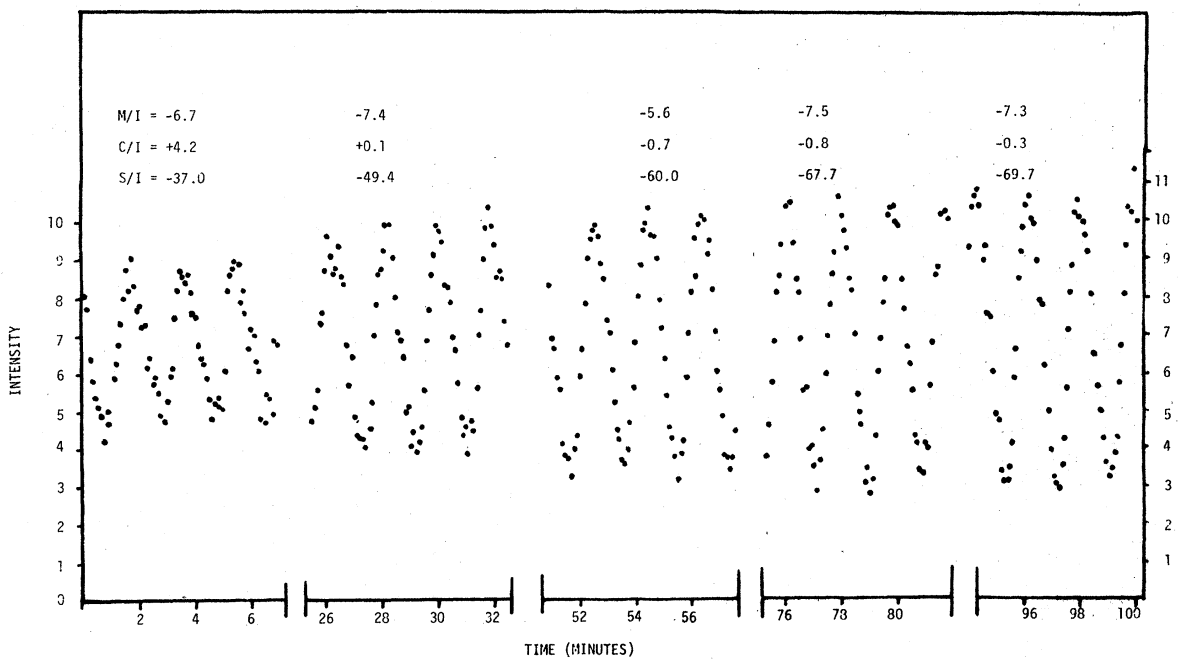

FIG. 13. Time dependence of the Stokes parameters of the ArII 4610-Å transition as a copper surface ($\alpha = 8°$) "cleans up" under Ar^+ bombardment. The observations are made at the down-beam end of the interaction region, and the final S/I (given as a percentage in the figure) corresponds to $S/I = 80$ % for the forward-scattered ions.

of wavelength. Such measurements support our conclusions above, that only the fast ions emitted at small grazing angles have high S/I.

In Fig. 15, we show the variation of the Stokes parameters with wave-length for the two tilt angles $\alpha = 1.5°$ and $\alpha = 8°$ observed just down beam from the interaction region. We have used an observation direction $\phi = 60°$ to obtain both a wavelength shift (zero at $\phi = 0°$, maximum at $\phi = 90°$) and a circular-polarization measurement ($S/I = 0$ at $\phi = 90°$, and is a maximum at $\phi = 0°$). For $\alpha = 1.5°$, there is almost no variation in the Stokes parameters, confirming that almost all ions are emitted near the specular direction. For $\alpha = 8°$, the linewidth was larger, confirming the larger velocity and angular distribution, and the high Doppler-shift components (at low wavelengths), from ions of larger scattering angles, show lower S/I. These results are only qualitative because ions of very large scattering angle which are expected to have very low velocities would also give small Doppler shifts. These ions may contribute to the falloff in S/I at the high wavelengths. However, at both ends of the wavelength region there may be some blending from other ArII transitions (of the same multiplet) which tend to reduce S/I values.

An attempt to observe the Stokes parameters for these ions in the interaction region resulted in the unexpected reversal in sign of S/I at high wavelengths shown in Fig. 16. We attribute this result to the reflection of photons in the shiny copper surface. The light is initially emitted in the opposite direction, thus having the opposite circular polarization and a Doppler shift to the red. Both these effects are exactly what is needed to produce the results of Fig. 16, but made it impossible to study the velocity distributions at the surface directly.

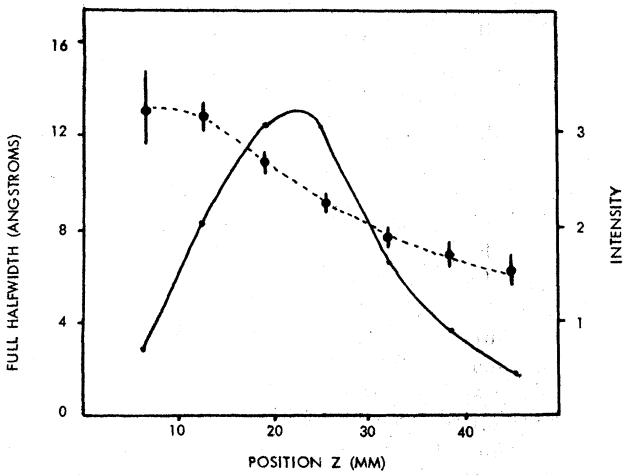

FIG. 14. Linewidth (points and dashed line) of the ArII 4610-Å transition as a function of position along the beam axis (Z). The incident ion energy is 1.0 MeV and the interaction region is at $15 \leq Z \leq 25$ mm as can be seen from the total intensity curve (solid line).

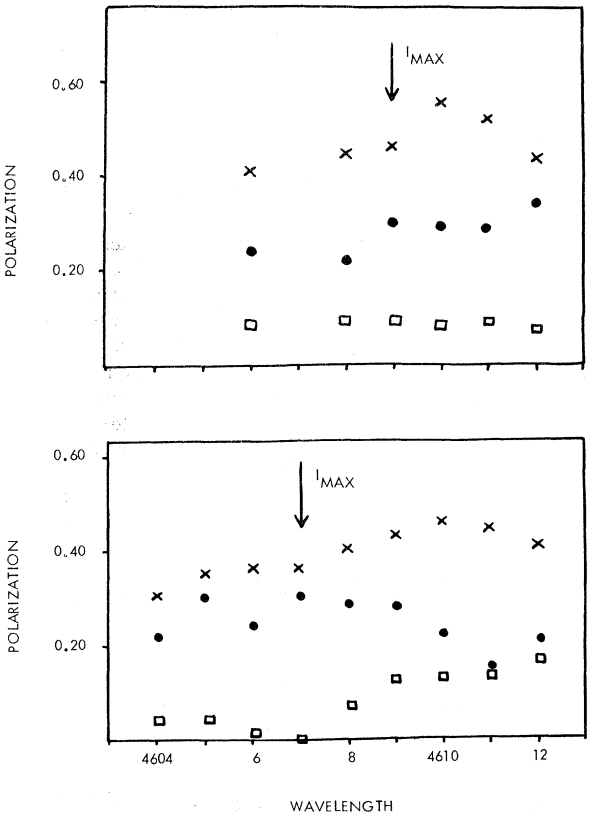

FIG. 15. Wavelength dependence of the Stokes parameters of the Ar II 4610-Å transition from forward-scattered Ar^+ ions viewed at $\phi = 60°$. The incident ion energy is 1.0 MeV with a copper surface of grazing angle $\alpha = 1.5°$ (upper) and $\alpha = 8°$ (lower). The crosses (×) are the circular polarization S/I, the points (●) and squares (□) the linear polarizations M/I and C/I, respectively. The wavelength of maximum intensity is also shown, the halfwidth being similar to that shown in Fig. 16.

In conclusion, the Doppler measurements are only able to give qualitative support to our interpretation of the spatial distribution of orientation and alignment and the ion-velocity distributions.

VI. SPUTTERED IONS

Light was observed from both neutral and singly ionized sputtered particles of Cu, Au, and Al. The velocities are low compared with those of the scattered ions. Thus, the light output was localized very close to the surface interaction region and was useful in verifying the spatial coordinates of the interaction. Also the linewidths were very small. The Al I 3966-Å transition was measured to have a linewidth of 1.2 Å, which corresponds to particle energies of about 500 eV.

A spatial distribution mapping of the Stokes parameters of the Cu II 4651-Å transition showed very low polarization fractions with S/I, $C/I \leq \pm 0.02$ and $M/I = -0.06 \pm 0.02$, which were independent of viewing position. Our results show that ions emitted at low velocities from surfaces have very little alignment or orientation at all angles.

VII. OBSERVATIONS OF OTHER TRANSITIONS AND COMPARISONS WITH TILTED-FOIL EXCITATION

It has been shown previously[1,2] that many Ar II transitions show strong circular-polarization fractions, especially in the forward-scattered distribution.[2] Although blending is a severe problem for many of the Ar II transitions, these results showed that the orientation fraction $\overline{O}_{1-} = \langle L_x \rangle / [L(L+1)]^{1/2}$ defined in Eq. (4) is approximately constant. The constancy of $\overline{O}_{1-}$ for different multiplets shows that the orientation production mechanism is not sensitive to the excited-state wave functions. The constancy of $\overline{O}_{1-}$ for different components within a multiplet indicates that the interaction is spin independent as expected.[24]

The measured sign of the orientation parameter $\overline{O}_{1-}$ gives a direction of spin of the scattered ion into the surface for all observed transitions of scattered ions of Ar II[1,2] and in Ne II–IV , He I, II and N II . We have also measured circular-polarization fractions (work to be published) for many transitions in these ions excited by thin foils, and they indicate the same sign of the orientation parameter $\overline{O}_{1-}$. This is further evidence that the final-state ion-surface interaction produces the orientation for both thin-foil and surface excitation of fast ions.

Less complete mappings of the spatial dependences of the Stokes parameters have been made for the He II $n = 3-4$ and $n = 3-5$ transitions for 1-MeV He^+ incident on Au, Cu, and Al surfaces, and for the Ne II 3230-Å and Ne III 2866-Å transitions for 1-MeV Ne^+ incident on Au surfaces. The spatial dependences are similar to those shown for Ar II 4610 Å in Figs. 5–7, showing the dependences are quite general, and probably are as independent of energy as the total ion angular distributions. No careful comparisons of the spatial dependences of Stokes parameters for transitions arising from different charge states under the same interaction conditions have been made.

The charge-state distribution as a function of scattering angle, which was not measured in these experiments, could provide a measure of the final velocity distribution if it can be compared directly with the charge states produced in thin-foil excitation. These are known, e.g., from the work of Moak *et al.*,[25] for thin carbon foils at 0° incidence and exit angles, but a few measurements have been made for exit angles away from the surface nor-

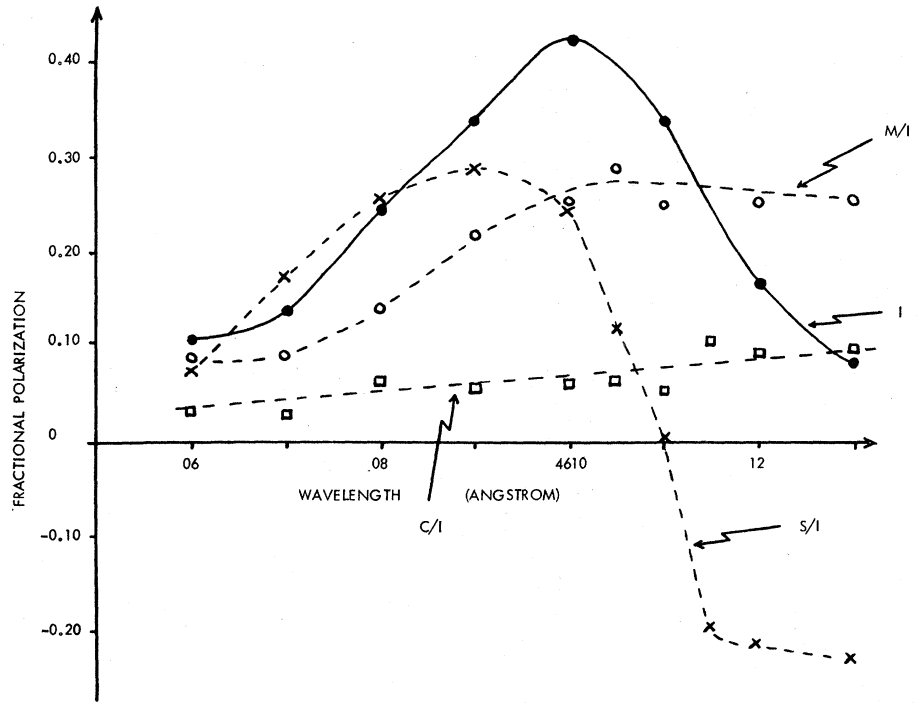

FIG. 16. Stokes parameters observed from ions near the interaction surface as functions of wavelength for the Ar II 4610-Å transition. The emission angle is $\phi = 60°$, with incident Ar^+ energy of 1.0 MeV and surface tilt angle $\alpha = 3°$.

mal. Thus, Chateau-Thierry and Gladieux[26] have shown that hydrogen at 1.4 MeV energy has a higher net charge at higher exit angles (away from the normal) as opposed to the low energy results of Hagstrum[27] who showed that for ions of a few keV energy, more neutralization occurs for increasing exit angles. Theoretical models of charge-state distributions assume a final-state charge capture at the surface. From this interpretation we should expect foil- and surface-scattered distributions to be the same for a given ion velocity and exiting angle. Kitagawa and Ohtsuki[28] have generalized the charge-capture model of Trubnikov and Yablinski[29] and explain qualitatively the angular dependences of the charge-state distributions. However, they include only the effect of tunneling of electrons from a static "jellium" potential to the outgoing ion. They neglect the dynamic effects of changes in the bulk and surface due to the ion motion and other important charge-changing effects such as autoionization and recombination processes.

VIII. CONCLUSIONS

We have measured the Stokes parameters of light emitted from surface-scattered ions both as functions of the spatial distribution of the ions relative to the interaction region, and also for different photon emission angles for a given position. We were thus able to investigate the alignment and orientation of the excited ionic state as a function of scattering angle.

We have shown that the alignment and orientation parameters of ions scattered from metal surfaces depend strongly on the angle of emission from the surface. For fast ions undergoing forward scattering close to the surface, the alignment is small except in the direction perpendicular to the plane of the beam velocity and surface normal. The orientation, which is in this same $\hat{n}\times\hat{v}$ direction, is close to the maximum possible for the state of measured small alignment.

We are able to interpret all the data of the optical experiments by associating the excited-state production with a final-surface interaction as the ions leave the surface. Such an interaction could be an electron pick-up from a bound state in the solid through a surface-tunneling mechanism, or from free electrons liberated from the surface by the collision, or electrons on the exiting ion could be excited directly by the surface. Our experiments cannot clearly differentiate these three modes of excitation, which probably all occur. The mechanism which produces the strong orientation is enhanced for clean metal surfaces over dirty surfaces.

The total ion-scattering distrubution is peaked close to, but just below, the specular scattering angle, and shows qualitative agreement with the multiple-scattering theory of Firsov. The major discrepancies are the angle of the maximum of the ion distribution and the stronger scattering

observed at higher angles.

Our results indicate that the excitation can be parametrized in terms of the velocity and direction of the ion as it leaves the surface. In this way the excitation is similar to the excitation of ions which pass through thin tilted foils. Exact comparison has not been possible because of the lack of clean metallic foils. However, we do find qualitative agreement between the orientation production by thin tilted foil and by grazing surface excitation. In both cases for all transitions observed, the sign of the orientation parameter is the same and increases monotonically to a maximum as the exiting-ion direction becomes closer to the surface. The well-defined velocity and direction of excited foil ions should allow more quantitative investigation of the angle and velocity dependence of the surface interaction.

Finally, we also find that sputtered ions have no orientation, a further indication of the symmetric distribution of the energy in sputtered particles about the surface normal.

ACKNOWLEDGMENTS

We thank Bob DeSerio, Tim Gay, Jim Ray, and Jim Stadelmann for their help in the measurements, and Murray Peshkin for helpful discussions of the theory.

---

*Supported in part by U. S. ERDA and NSF.

[1]H. J. Andrä, Phys. Lett. 54A, 315 (1975); H. J. Andrä, R. Fröhling, H. J. Plöhn, and J. D. Silver, Phys. Rev. Lett. 37, 1213 (1976); H. J. Andrä, H. J. Plöhn, A. Gaupp, and R. Fröhling, Z. Phys. 281, 15 (1977).

[2]H. G. Berry, G. Gabrielse, A. E. Livingston, R. M. Schectman, and J. Desesquelles, Phys. Rev. Lett. 38, 1473 (1977).

[3]M. Hass, J. M. Brennan, H. T. King, T. K. Saylor, and R. Kalish, Phys. Rev. Lett. 38, 218 (1977); G. Goldring, Y. Niv, Y. Wolfson, and A. Zemel, Phys. Rev. Lett. 38, 221 (1977).

[4]E. S. Mashkova and V. A. Molchanov, Radiat. Eff. 16, 143 (1972).

[5]E. Veje, Phys. Rev. A 14, 2077 (1976).

[6]H. G. Berry, J. Bromander, and R. Buchta, Nucl. Instrum. Methods 90, 269 (1970); see also: R. D. Hight, R. M. Schectman, H. G. Berry, G. Gabrielse, and T. Gay, Phys. Rev. A 16, 1805 (1977).

[7]H. G. Berry, L. J. Curtis, D. G. Ellis, and R. M. Schectman, Phys. Rev. Lett. 32, 751 (1974).

[8]H. G. Berry, G. Gabrielse, and A. E. Livingston, Appl. Opt. (to be published).

[9]V. A. Arifov, *Interaction of Atomic Particles with a Solid Surface* (Plenum, New York, 1969), pp. 116–120.

[10]E. S. Mashkova and V. A. Molchanov, Radiat. Eff. 13, 133 (1972).

[11]R. J. MacDonald, Adv. Phys. 19, 457 (1970).

[12]S. Datz and C. Snoek, Phys. Rev. 134, 347 (1964); P. Dahl and N. Sandager, Surf. Sci. 14, 305 (1969).

[13]E. S. Parilis and N. Y. Turaev, Dokl. Akad. Nauk SSSR 161, 84 (1965) [Sov. Phys. Dokl. 10, 212 (1965)].

[14]V. M. Kivilis, E. S. Parilis, and N. Y. Turaev, Dokl. Akad. Nauk SSSR 173, 805 (1967) [Sov. Phys. Dokl. 12, 328 (1967)].

[15]W. Heiland and E. Taglauer, Nucl. Instrum. Methods 132, 535 (1976).

[16]O. B. Firsov, Dokl.Akad. Nauk SSSR, 169, 1311 (1966) [Sov. Phys. Dokl. 11, 732 (1967)].

[17]O. B. Firsov, Fiz. Tverd. Telz (Leningrad) 9, 2145 (1967) [Sov. Phys. Solid State 9, 1687 (1968)].

[18]E. S. Mashkova and V. A. Molchanov, Dokl. Akad. Nauk. SSSR 146, 585 (1962) [Sov. Phys. Dokl. 7, 829 (1963)].

[19]G. G. Stokes, Trans. Camb. Philos. Soc. 9, 399 (1852).

[20]D. G. Ellis, J. Opt. Soc. Am. 63, 1232 (1973).

[21]U. Fano and J. H. Macek, Rev. Mod. Phys. 45, 553 (1973).

[22]H. G. Berry, Rep. Prog. Phys. 40, 155 (1977).

[23]J. O. Stoner Jr. and J. A. Leavitt, Appl. Phys. Lett. 18, 477 (1971).

[24]D. G. Ellis, J. Phys. B (to be published).

[25]C. D. Moak, L. B. Bridwell, H. O. Lutz, S. Datz, and L. C. Northcliffe, *Beam-Foil Spectroscopy I*, edited by S. Bashkin (Gordon and Breach, New York, 1968), p. 157.

[26]A. Chateau-Thierry and A. Gladieux, *Atomic Collisions in Solids*, edited by S. Datz, B. R. Appleton, and C. D. Moak (Plenum, New York, 1975), p. 307.

[27]H. D. Hagstrum, Phys. Rev. 96, 336 (1954).

[28]M. Kitagawa and Y. H. Ohtsuki, Phys. Rev. B 13, 4682 (1976).

[29]B. A. Trubnikov and Y. M. Yablinski, Zh. Eksp. Teor. Fiz. 52, 1638 (1967) [Sov. Phys. JETP 25, 1089 (1967)].